

Petrology, Geochemistry, and Geodynamic Implications of Basaltic Dyke Swarms from the Southern Continental Part of the Cameroon Volcanic Line, Central Africa

Jean Pierre Tchouankoue, Nicole Armelle Simeni Wambo, Armand Kagou Dongmo and Gerhard Wörner*

Abt. Geochemie, GZG, University Goettingen, Germany

Abstract: Basaltic dyke swarms in the southern continental part of the Cameroon Volcanic Line (Bangangte, Dschang, Manjo areas) are tholeiitic in composition with 46 to 50 wt.% SiO₂ and have moderate Mg-numbers (53–59), medium TiO₂ contents (1.48–2.05 wt.%), and flat to mildly enriched incompatible trace element patterns. Comparison with trace element patterns of representative Cenozoic basaltic rocks of the Cameroon Volcanic Line (Bana anorogenic complex, Mt. Bambouto, Adamawa Plateau basalts) indicates that these dykes are less enriched in light REE and show different incompatible trace element ratios (La/Yb: 5.7 to 8.6; Zr/Nb: 7.6 to 12.0; Ba/Th: 87.7 to 93.3). The trace element patterns of the dykes and their Sr- and Nd- isotope compositions, however, are similar to those of the pre-Cenozoic volcanic rocks of the Benue Trough in Nigeria. Our data therefore suggest that these dykes represent the magmatic history related to the break-up of Africa and South America and are unrelated to the Tertiary volcanism of the Cameroon Line.

Keywords: Basalt dykes, Tholeiites, Phanerozoic, Cameroon volcanic line, West Gondwana.

INTRODUCTION

Mafic magmatic dykes are important in the characterization and the reconstruction of the tectonomagmatic history of a region. Basalt dykes of the continental part of the Gulf of Guinea in Central Africa are abundant and - if they can be safely differentiated from dikes related to the Cameroon Volcanic Line (CVL)- may be good candidates for a better understanding of the break-up of the Pangea supercontinent during the Mesozoic.

In the present work, we report mineral chemistry, whole rock geochemistry, and Sr- and Nd-isotopes for 12 basaltic dykes that cut the Precambrian rock assemblages outcropping below the Tertiary volcanic cover of the Cameroon Volcanic Line (CVL) in the areas of Bangangté, Dschang and Manjo (Fig. 1). We compare the trace element patterns of these basalt dykes with the CVL plateau basalts from the Bangangte area (this work), basalts from the Cenozoic Bana anorogenic complex [1], Mt. Bambouto and Ngaounderé plateau basalts [2], as well as basalts from the Benue Through in Nigeria [3].

[4] and [5] on their reconnaissance 1/500000 map of Cameroon recognized the existence of dykes of basaltic affinity within the corridor of the Cameroon Volcanic Line. Poorly constrained K/Ar ages (417 ± 8.1 Ma; 214 ± 6.6 and $148. \pm 3.8$ Ma respectively, for two such mafic dykes in the Bangangte area [6] indicate that these basalts could be related to the opening of the South Atlantic Ocean and less likely to initial stages of the building up of the Cameroon

Line. These K-Ar ages added to the interest in these basaltic dykes in the perspective of the geodynamic history of the opening of Central Atlantic.

We will use our new geochemical and isotopic data on mafic basement-cutting dikes in south-central Cameroon to (1) better differentiate between products Lower Tertiary CVL magmatism and older dykes that formed within the context of Phanerozoic magmatism linked to the opening of the South Atlantic Ocean, and (2) characterise the magmatism during the opening of the Central Atlantic.

GEOLOGICAL SETTING

The Precambrian domain of southwestern Cameroon is a part of the Pan-African belt of Central Africa north of the Congo Craton which was formed following the convergence and collision between the Congo-São Francisco cratons, the West African craton and a Pan-African mobile belt ([7-10]).

The tectono-magmatic history of the domain includes a Panafrican massive granitization event [15, 16], the opening of the Central Atlantic during the Mesozoic, and the formation of the Cameroon Volcanic Line during the Tertiary. Basaltic dykes are found cutting across the Precambrian basement that is mainly formed by syn- to late-tectonic granitoids intruded into a gneissic basement [10-14]. Granitoids appear as sheets elongated aggregately to the N30-40°E direction. Plutons are parallel to the regional schistosity with planar structures of mean attitude N45-70°SE. Petrographically, granitoids are fine- to coarse-grained types (granites, granodiorites, monzogranites, granites, syenites) and intrusive massifs are frequently formed by more than one rock type. Amphiboles and biotite form the dominant mafic minerals and muscovite, monazite

*Address correspondence to this author at the Abt. Geochemie, GZG, University Goettingen, Germany; Tel: 0049 551 393971; Fax: 0049 551 393982; E-mail: Gwoerne@gwdg.de

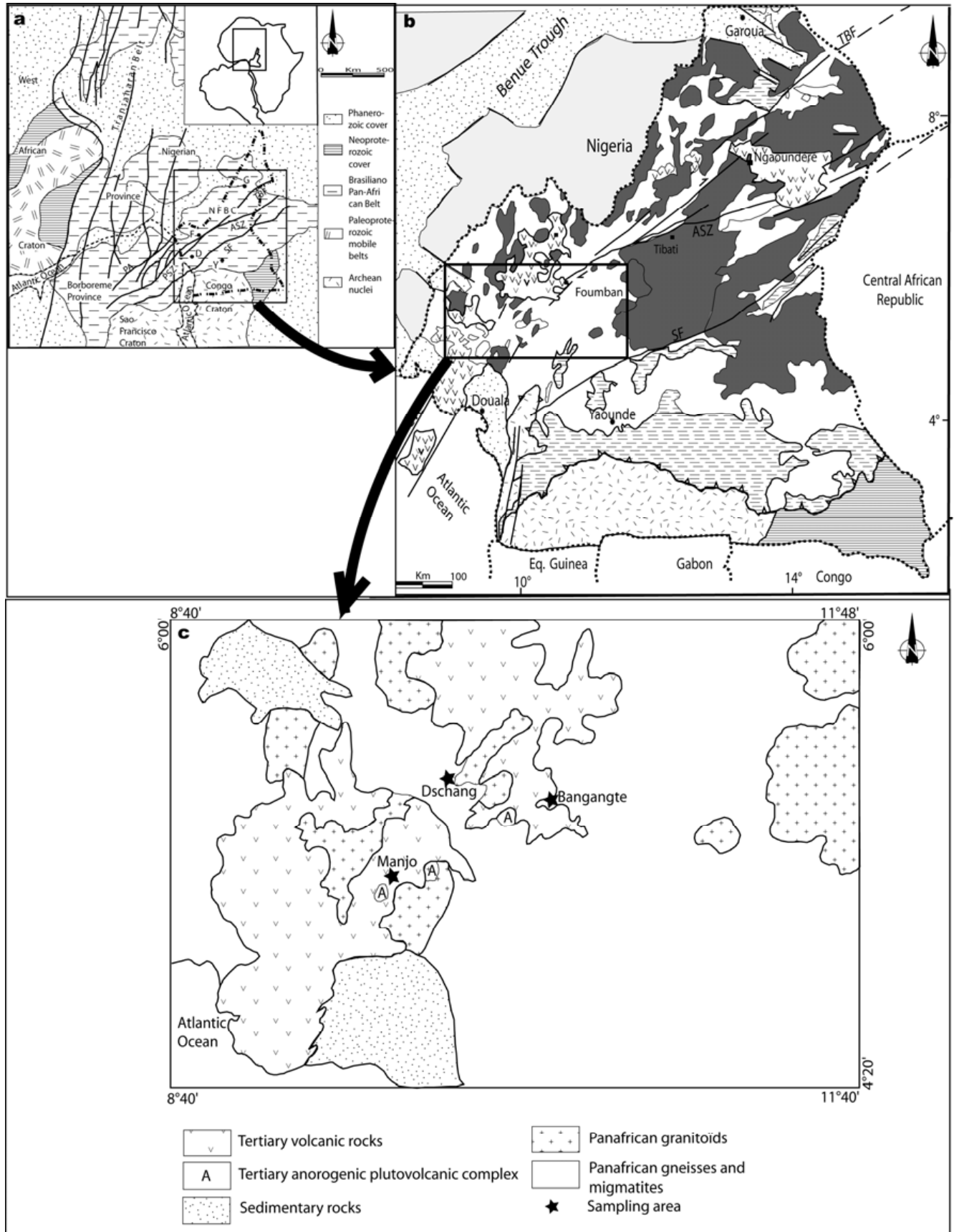


Fig. (1). (a) Position of Cameroon in West Gondwana assembly and (b) geology map of Cameroon (in [10]). (c) Geological sketch map and samples location.

and hypersthene are found in some cases. Granitoids as well as gneissic rocks share common geochemical characters: I-type, high-K calcalkaline compositions.

Geochemical data on mafic dykes in the corridor of the Cameroon Volcanic Line exists only for the Mt. Cameroun area where they show lamprophyritic compositions (camptonites and monchiquites) and are clearly related to the alkaline magmatism of the Cameroon Volcanic Line [17]. Other occurrences are in the area of Benoue River in North Cameroon and the Adamawa plateau. In all these cases, they were inferred to be contemporaneous with and related to the nearby CVL alkali basalts [17-19]. The lamprophyres have high incompatible element contents and contain hydrous (kaersutite, biotite) and/or carbonate minerals and are interpreted to originate from a volatile-rich metasomatized lithospheric mantle [20]. In the Adamawa region, however, dykes are mainly doleritic [21]. Although undated, these dolerites with continental tholeiitic affinities are thought to be older since they were never found to crosscut the 51 Ma plateau basalts of the early CVL units. Thus, they may not be related to the CVZ at all but rather may be linked to different magma sources and a distinct tectonic setting. Principal directions between 30°E and 70°E of these generally nearly vertical dykes are consistent with main characteristics of brittle deformation in the studied area [22] and indicate that a pre-Gondwana break-up (Panafrikan) network of faults may have guided the ascent of these dykes to the surface.

ANALYTICAL METHODS AND TECHNIQUES

Twelve samples were selected for this study. Data are shown on Table 4.

Mineralogical and geochemical studies were carried out at the University of Göttingen. Clinopyroxenes, amphiboles and biotite were analysed by electron probe micro-analyzer (EPMA) at the University of Göttingen using a JEOL X-8900 electron microprobe equipped with a wavelength dispersive analytical system. Operating conditions were 15kV and 12 nA using a focused beam at counting times of 10 seconds. ZAF-corrections were made using atomic number, absorption and fluorescence incorporated routine methods.

Major and trace elements were determined using a Philip-PW 1408 XRF spectrometer. Analyses were carried out on lithium borate glass fusion beads. Relative precision (2 Σ) for repeated measurements of standards is generally better than 2% for the major oxides and better than 10 % for trace elements. Rare Earth and trace elements were analysed by inductively coupled plasma mass spectrometry (ICP-MS) on a VG-Plasma Quad STE-ICP mass spectrometer. The samples were dissolved in a Teflon pressure bomb, using a 1:1 mixture of HF and HClO₄ at 180°C, and then taken up in an HNO₃ solution with an In-Re international standard. After dissolution in HF-HClO₄, the samples were taken up in a mixture of HNO₃, 6N HCl and Hf and diluted. These solutions were measured within 24 hours after dilution to prevent absorption of HFSE. Isotope ratios for Sr and Nd were measured with a Finnigan MAT 262 RPQ II+ mass spectrometer at Göttingen. Whole-rock powders (ca. 100 mg) were dissolved in HF/HNO₃. The Sr and Nd-isotope ratios were corrected for mass fractionation to $^{86}\text{Sr}/^{88}\text{Sr} = 0.1194$ and $^{146}\text{Nd}/^{144}\text{Nd} = 0.7219$ and normalized to values

for NBS987 (0.710245), and La Jolla (0.511847), respectively. Measured values of these standards over the last 3 years in Göttingen were 0.710239 ± 0.000004 for Sr and 0.511844 ± 0.000003 for Nd. External errors (2r) are estimated at $\pm 0.0004\%$ for Sr and Nd isotopes. Procedural blanks for Sr and Nd (261 and 135 pg respectively) were negligible.

FIELD CHARACTERISTICS AND PETROGRAPHIC DESCRIPTIONS

Within the sampling area, dykes are irregularly distributed. Taking into account the intense weathering of rocks that characterizes the region, great care was taken to collect only relatively fresh samples from outcrops along highways at Bangangté and Dschang, and in a quarry near Manjo (Fig. 2). Basalt dykes in the studied area only intrude the Precambrian basement and never into Tertiary plateau basalts.

Rose and density diagrams for strike and dip of 12 dykes (Fig. 3) indicate major orientations directions between 30°E and 70°E and near vertical dip; the two dykes oriented N100°E and N150°E are located in the Dschang area. Many dikes are intensely internally fractured with reflecting no systematic (and presumably rather local) stress patterns.

Dschang Area

Six dykes have been identified within the Precambrian host rock assemblage, along the escarpment west of the city of Dschang. Dyke emplacement occurred with development of numerous apophyses and intense brittle fragmentation of the country rocks (Fig. 2d, e). Rocks show remarkable uniform subophitic texture (Fig. 4d) with large phenocrysts of olivine and plagioclases representing 25 vol.% of the rock. The groundmass is comprised of plagioclase, micrograins of olivine, augite and Fe-Ti-oxides. One dyke shows locally variations to a fluidal texture underlined by smaller laths of plagioclase. Both plagioclase and olivine phenocrysts are frequently altered.

Manjo Area

Three basalt dykes from a quarry at 5 km to the north of the city of Manjo show thicknesses varying between 0.3 and 0.65 m (Fig. 2c). Dykes are homogeneous with intragranular to interstitial, subophitic texture (Fig. 4c, d): Primary minerals include augite, hypersthene, plagioclases, minor biotite, and rare zircons. Secondary minerals are amphibole, biotite, and calcite. Plagioclase occurs as large laths varying in length between 0.5 and 1.5 mm. Saussuritization of plagioclase is frequent with formation of epidote, sericite and often calcite. Augite phenocrysts are frequently replaced by secondary fibrous green hornblende. Small flakes of biotite can form from some pyroxenes, but biotite is also found as small plates with diameters below 0.1mm.

Bangangté Area

In the Bangangté area, three dykes were studied: two basaltic dykes located 10km [11] to the north-west of the city of Bangangté (Bangwa) and one dyke at 25km to the south-east of the city (Maham). Thicknesses of the dykes vary from 1.20 m in the Maham area (Fig. 2a) to 20 cm in the Bangwa area (Fig. 2b). Basaltic dykes at Bangwa are porphyritic, with olivine and plagioclase phenocrysts in a

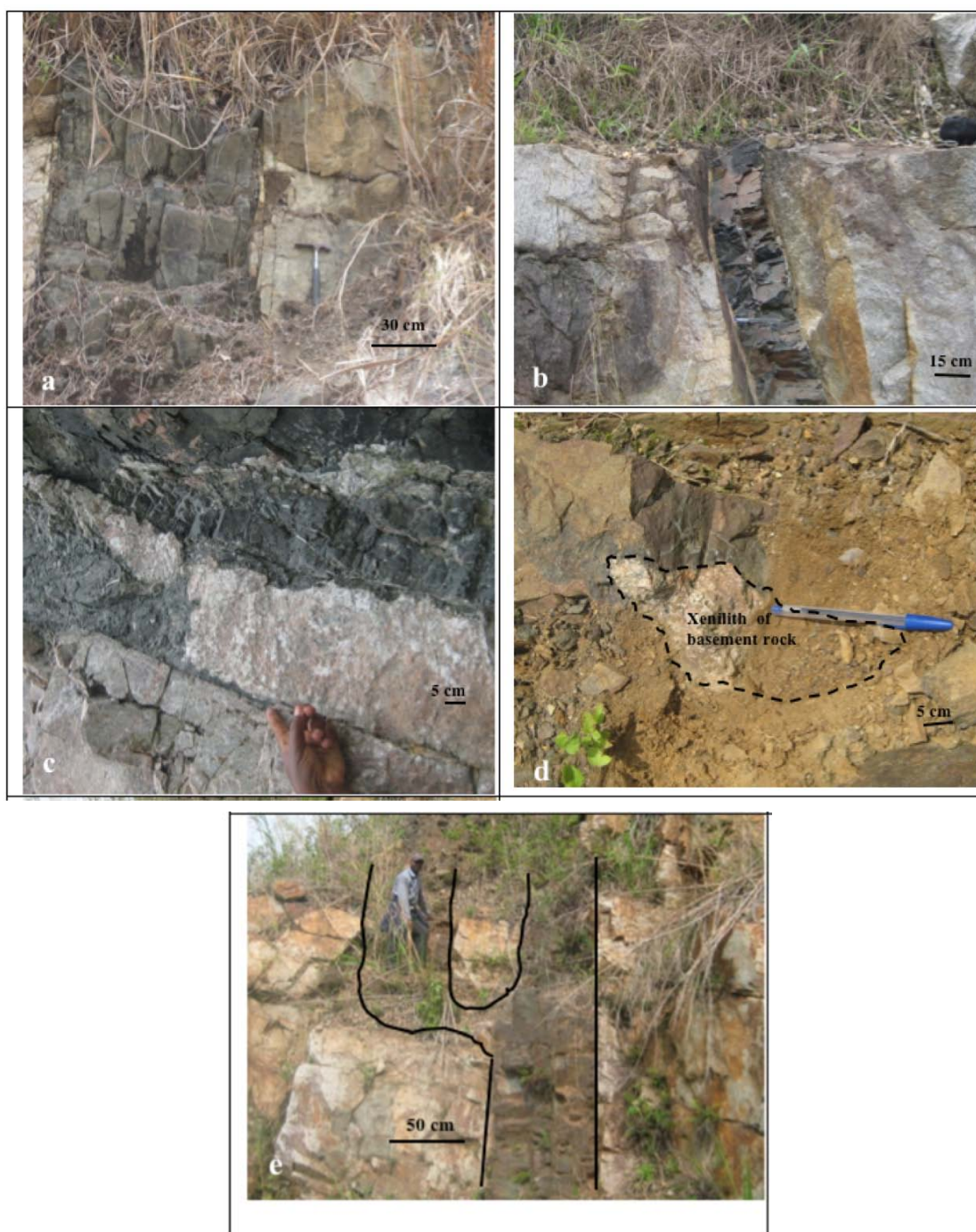


Fig. (2). Front view of basalt dykes. Intense fracturation and large variations of dykes sizes in the Bangangte area (**a**, **b**); dike in contact with country rock at Manjo (**c**). Note fragmentation and thin basaltic injection into fissures of the host rock. Blocks of basement included as fragments and xenoliths in Dschang dykes (**d**, **e**).

matrix made up of plagioclase, olivine, augite, and chromite microlites (Fig. 4b). Xenoliths minerals (quartz, amphiboles) of basement rocks are frequent at Bangwa (Fig. 4c). In the Maham area the porphyritic dykes depict a clear fluidal texture at the contact with the gneissic basement and glassy selvages at the sharp contacts with the country rocks (Fig. 4a).

MINERAL CHEMISTRY

Clinopyroxenes, and biotite, amphiboles, plagioclases were analysed by electron microprobe. Clinopyroxene

phenocrysts are relatively abundant compared to olivines which are mostly affected by alteration. Data are shown in Table 1. Clinopyroxenes are diopside to augite in composition (Fig. 4d, 5) according to the classification of [23] with compositions in the range $Wo_{49-43}En_{32-43}Fs_{12-24}$. Clinopyroxenes in the Bangangte and Dschang areas are augites and diopside in the Manjo area. Based on the amount of Ti and Ca, clinopyroxenes can be distinguished and classified as titaniferous calcic clinopyroxene (Bangangté and Dschang area) and weakly non-titaniferous calcic-

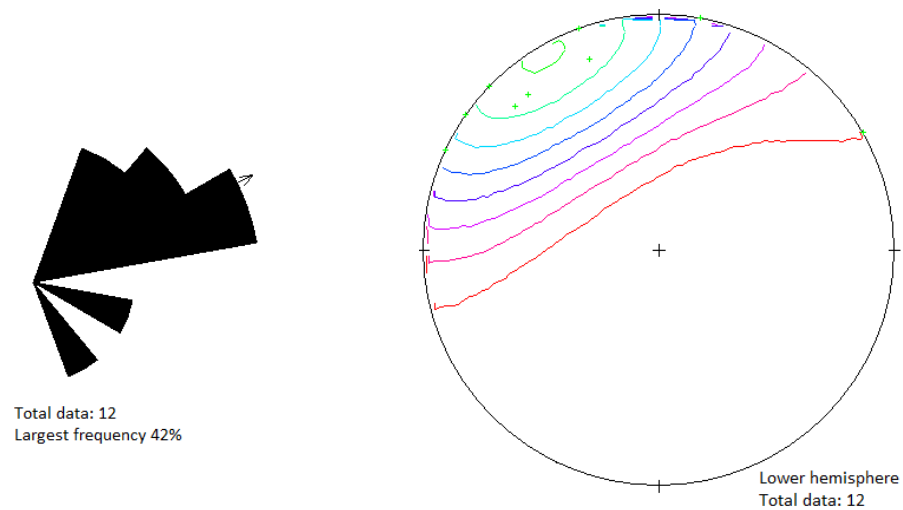


Fig. (3). Rose diagram and poles of dykes. Most dykes are oriented between N30 and N70°E with near to vertical dips.

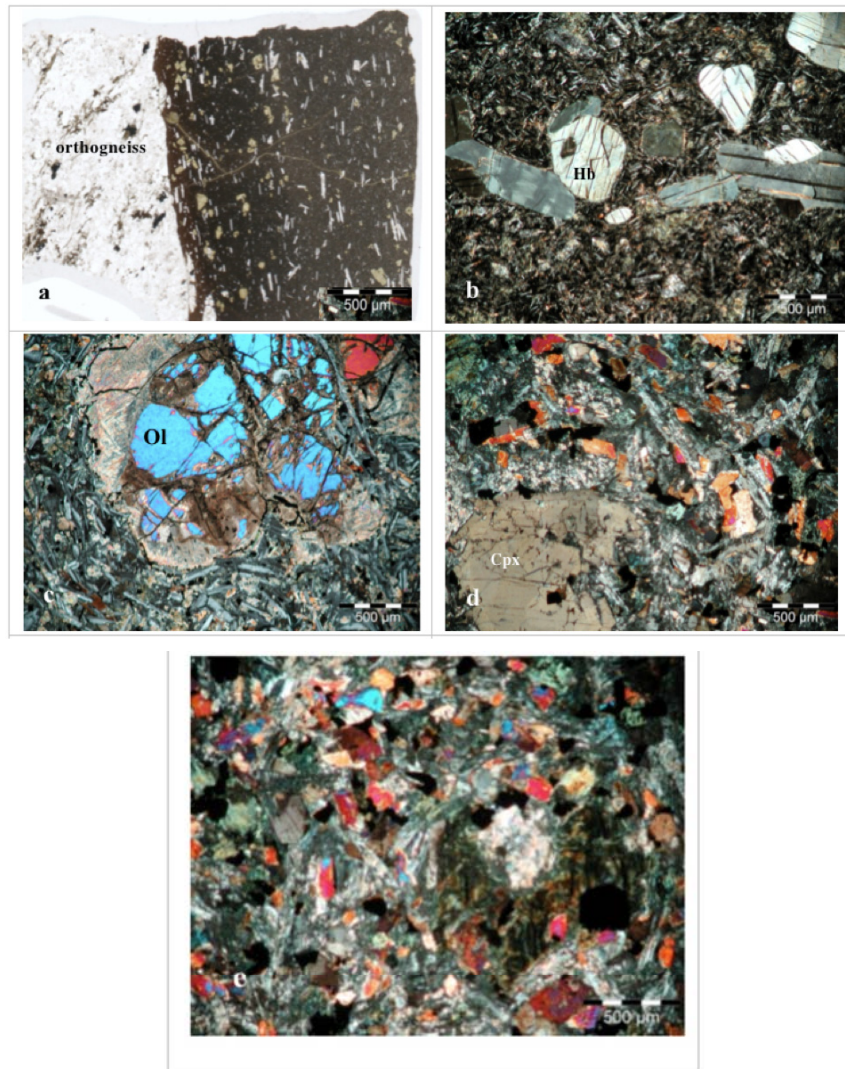


Fig. (4). Photomicrographs showing main textural characteristics of the dykes (a) Fluidality in the microlitic texture of near the contact with bed rock (orthogneiss) of dyke a on Fig. (2). Sharp contacts indicate that the dyke was put in place along a preeexisting fracture. (b) xenoliths (quartz, green hornblende) of the basement rocks in dyke 2-B. (c) microlitic porphyritic textures and intense alteration of olivines in a dykes of the Dschang area. (d, e) microlitic porphyritic textures and hydrous minerals (green hornblende, biotites) in dykes of the Manjo area. Ol, Olivine ; Cpx, Clinopyroxene ; Hb, Green Hornblende.

Table 1. Selected Electron Microprobe Analyses of Clinopyroxenes

wt%	DMA1 1	DMA1 2	DMA1 3	FBBI 3	FBBI 5	FBBI 7	FFD2A-9	FFD2A-8	FFD2A	FFD2A-1	FFD2A-2	FFD2A-3	FeM3-2	FeM3-3	FeM3-4	FeM3-5	FeM311	FeM312	FeM313	FeM3 14	FeM315	FeM3 16	FeM317
SiO ₂	52.81	52.18	52.05	46.47	46.42	46.87	46.21	45.16	46.38	46.98	46.51	47.13	50.77	45.41	46.03	49.00	49.83	45.93	45.53	45.94	50.04	46.06	44.17
TiO ₂	0.04	0.14	0.16	2.71	3.01	2.81	2.93	3.31	2.80	2.75	2.94	3.01	1.12	3.05	3.22	1.86	1.62	2.35	2.94	2.85	1.48	3.01	4.12
Al ₂ O ₃	0.88	1.56	1.53	5.53	5.45	5.80	4.75	5.43	4.74	4.66	4.44	4.82	2.39	7.25	6.50	4.21	3.92	8.84	7.19	7.25	3.93	7.16	8.62
Cr ₂ O ₃	0.05	0.03	0.01	0.21	0.16	0.23	0.16	0.23	0.10	0.17	0.17	0.07	0.00	0.00	0.01	0.01	0.05	0.61	0.01	0.11	0.09	0.01	0.03
FeO	10.92	11.16	11.02	11.55	13.02	11.49	12.72	11.83	13.33	12.71	13.47	12.96	10.79	9.33	9.20	8.19	7.69	6.70	9.21	7.95	7.27	8.93	9.50
MnO	0.55	0.49	0.57	0.24	0.24	0.23	0.27	0.25	0.30	0.22	0.28	0.29	0.28	0.13	0.20	0.18	0.18	0.15	0.20	0.10	0.17	0.13	0.15
MgO	12.12	11.79	11.93	11.59	10.86	11.73	10.52	10.41	10.77	10.68	10.62	10.80	12.30	11.57	11.35	13.58	14.37	12.84	11.56	12.45	14.51	11.90	10.85
CaO	22.93	22.21	22.07	19.85	19.08	19.82	20.21	20.39	19.60	20.19	19.57	20.04	21.69	21.59	21.55	21.53	21.38	21.09	21.56	21.89	21.42	21.56	21.53
Na ₂ O	0.44	0.55	0.57	0.36	0.60	0.42	0.50	0.44	0.48	0.50	0.49	0.45	0.41	0.51	0.59	0.39	0.41	0.49	0.57	0.46	0.37	0.50	0.56
K ₂ O	0.00	0.00	0.02	0.04	0.03	0.13	0.01	0.01	0.01	0.01	0.00	0.01	0.02	0.01	0.01	0.01	0.01	0.01	0.00	0.01	0.02	0.01	0.01
NiO	0.02	0.03	0.03	0.03	0.03	0.00	0.00	0.00	0.01	0.03	0.00	0.00	0.00	0.00	0.00	0.00	0.02	0.00	0.00	0.04	0.03	0.00	0.01
Total	100.75	100.14	99.94	98.58	98.87	99.54	98.29	97.46	98.52	98.90	98.49	99.58	99.76	98.85	98.67	98.96	99.47	99.00	98.78	99.05	99.34	99.28	99.53
6 O per formula																							
Si	1.98	1.97	1.97	1.79	1.79	1.79	1.80	1.77	1.80	1.81	1.81	1.81	1.92	1.74	1.76	1.85	1.86	1.73	1.74	1.74	1.87	1.75	1.68
Ti	0.00	0.00	0.00	0.08	0.09	0.08	0.09	0.10	0.08	0.08	0.09	0.09	0.03	0.09	0.09	0.05	0.05	0.07	0.08	0.08	0.04	0.09	0.12
Al	0.04	0.07	0.07	0.25	0.25	0.26	0.22	0.25	0.22	0.21	0.20	0.22	0.11	0.33	0.29	0.19	0.17	0.39	0.32	0.32	0.17	0.32	0.39
Cr	0.00	0.00	0.00	0.01	0.00	0.01	0.01	0.01	0.00	0.01	0.01	0.00	0.00	0.00	0.00	0.00	0.00	0.02	0.00	0.00	0.00	0.00	0.00
Fe ²⁺	0.34	0.35	0.35	0.37	0.42	0.37	0.41	0.39	0.43	0.41	0.44	0.42	0.34	0.30	0.29	0.26	0.24	0.21	0.29	0.25	0.23	0.28	0.30
Mn	0.02	0.02	0.02	0.01	0.01	0.01	0.01	0.01	0.01	0.01	0.01	0.01	0.01	0.00	0.01	0.01	0.01	0.00	0.01	0.00	0.01	0.00	0.00
Mg	0.68	0.66	0.67	0.67	0.62	0.67	0.61	0.61	0.62	0.61	0.62	0.62	0.69	0.66	0.65	0.76	0.80	0.72	0.66	0.70	0.81	0.67	0.62
Ca	0.92	0.90	0.89	0.82	0.79	0.81	0.84	0.86	0.82	0.84	0.82	0.82	0.88	0.88	0.88	0.87	0.86	0.85	0.88	0.89	0.86	0.88	0.88
Na	0.03	0.04	0.04	0.03	0.04	0.03	0.04	0.03	0.04	0.04	0.04	0.03	0.03	0.04	0.04	0.03	0.03	0.04	0.04	0.03	0.03	0.04	0.04
cation sum																							
	4.01	4.01	4.02	4.02	4.02	4.01	4.02	4.02	4.02	4.02	4.02	4.02	4.01	4.01	4.03	4.02	4.02	4.02	4.03	4.03	4.01	4.03	4.03
endmembers																							
Wo	47.46	46.93	46.70	44.12	43.02	43.94	45.13	46.22	43.57	44.89	43.62	44.36	45.94	48.00	48.39	45.98	45.12	47.74	48.09	48.20	45.31	47.83	48.89
En	34.90	34.66	35.11	35.83	34.07	36.17	32.69	32.85	33.29	33.04	32.95	33.25	36.23	35.80	35.47	40.37	42.21	40.43	35.87	38.15	42.69	36.72	34.27
Fs	17.64	18.41	18.19	20.05	22.91	19.89	22.18	20.93	23.13	22.07	23.43	22.39	17.83	16.20	16.13	13.65	12.67	11.83	16.04	13.65	12.00	15.45	16.84

clinopyroxene (Manjo area). Amphiboles and biotites clearly secondary alteration products (Fig. 4e). Biotite crystals are euhedral (<1mm) and exist only in the dykes of the Manjo area. They are close to Annite composition. Amphiboles occur only in the Manjo area and are of Tschermakitic type.

When compared to phenocryst data from Cameroon Line volcanics and related dykes, augites are closer to those of the Bana transitional tholeiites with compositions in the range Wo₄₇₋₃₆En₃₅₋₄₀Fs₁₅₋₂₅ (Kuepouo *et al.*, 2006) than representatives of basalt dykes in North Cameroon with Wo₃₈₋₂₆En₄₂₋₅₄Fs₂₃₋₅₂ (Ngounouno *et al.*, 2001).

WHOLE ROCK GEOCHEMISTRY

The dykes have restricted SiO₂ content from 46.6 to 50.9 wt.% with lowest values in the Manjo area, MgO spanning 7.18-9.38 wt.% (Table 2). The magnesium number Mg# (=Mg/(Mg+Fe²⁺)), calculated on the basis of Fe₂O₃/FeO=0.10, varies from 53 to 59. K₂O+Na₂O is less than 4.4 wt%. Na₂O/K₂O ratio varies from 1.38 to 5.08, with the highest value coming from the Dschang area, which partly may be due to alteration effects. TiO₂ contents are between 1.36 and 2.62 wt.%, with highest values (up to 2.62 wt.%) found in the Manjo area. Highest Al₂O₃ values (17.04 wt.%) are also

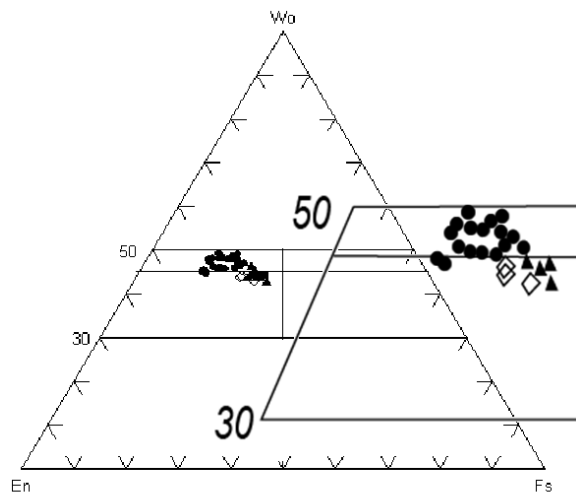


Fig. (5). Clinopyroxene compositions. Symbols: diamonds (Bangangte), triangles (Dschang), circles (Manjo). Data span the boundary between Diopside and Augite pyroxenes in Bangangte and Dschang areas are augites while pyroxenes in the Manjo area are diopside.

found in the Manjo area. Following the classifications of [24], and [25], all rocks are silica over-saturated subalkaline basalts (Fig. 6), with the exception of one dyke (FEM3) from the Manjo quarry which contains 7.5 wt.% of olivine, Variation diagrams for major elements show only small compositional ranges (Fig. 7).

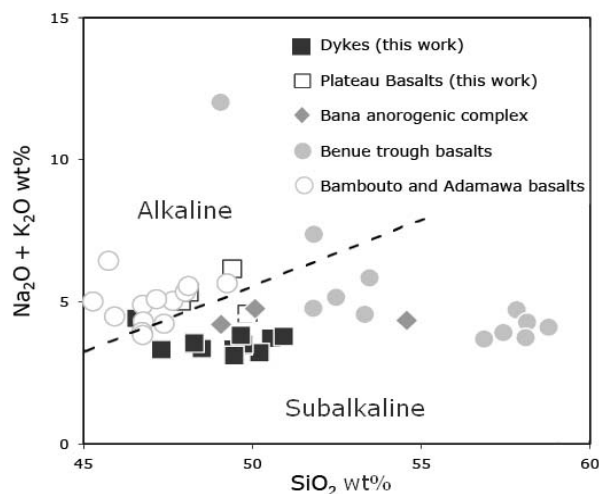


Fig. (6). Total alkali-Silica classification [24]. Dashed line delineates the boundary between alkaline and subalkaline basaltic series after [25]. Data source: Bana anorogenic complex [1]; Bambouto and Adamawa basalts [2]; Benue Through basalts [3].

Ratios of immobile incompatible elements (Fig. 8) should be largely independent of the degree of magmatic differentiation and also from secondary alteration effects and thus - if different, should indicate different magma sources.

Ratios such as Sm/Nd, Zr/Nb, Ba/Th, Th/La, Ba/La and Ba/Nb, K/Nb and REE patterns (Table 3, Figs. 9, 10) indicate that the dykes in the Bangangté and Dschang areas are similar, but slightly different from dykes in the Manjo area. Trace element patterns (Fig. 9) with concentrations normalized to chondrites compositions of [26] indicate relatively uniform enrichment in trace and rare earth elements, strong negative anomalies in Th and U, slightly positive anomalies in Nb, La and Y. In order to evaluate our data with possibly equivalent mafic volcanic rocks from the early stage of Cameroon Line magmatism in the area, we compared our trace element patterns with those of the Tertiary basalts from the Cameroon Volcanic Line. A comparison between the dykes and the basaltic rocks of the Cameroon Volcanic Line (see Fig. 9a, b), shows that trace element patterns and abundances are quite distinct: Large Ionic Lithophile Elements and Light Rare Earth Elements are lower in the basalt dykes as shown on Fig. (8). Further comparison is made with basalt rocks from the Benue Trough in Nigeria [3], which - as we will discuss below - bear many similarities to dyke rocks in Cameroon (Fig. 8).

Within the southern part of the Cameroon Volcanic Line, two dykes of basaltic affinity (camptonites) were described at Mount Cameroon (150 km to the SW of Manjo dykes area) by [17] that show some petrographic similarities with dykes of the Manjo area, i.e. the presence of minor amphiboles and biotites. However, major differences in their major and trace element geochemistry suggests that they are not related: The K_2O/Na_2O ratio of the Manjo dykes studied here are between 3 and 4 wt% while at Mt Cameroon these values are much higher (4.64 and 8.33 wt%). Incompatible trace elements patterns show positive K anomalies and negative anomalies for Th, U for the Manjo dykes which are not observed for the Mt Cameroon dykes. The isotopic compositions are also distinct and the Mount Cameroon dikes with a K-Ar age of 1.46 \pm 0.15 M are also much younger [17]. The Mount Cameroon camptonites are thought to represent the least differentiated basalts of the Cameroon Volcanic Line. Thus, in spite of the petrographic similarity (i.e. the presence of amphiboles and biotites) the dykes of Manjo and Mount Cameroon areas are distinct in age, composition, magma source and thus also in their tectonic setting.

Sr and Nd isotope data were obtained on a representative set of dyke samples. These were selected on the basis of their range in Sm/Nd and Rb/Sr ratios. Since no (reliable) chronological data exist on the dike rocks, calculation of initial isotope ratios is poorly constrained. We used an age of 150 Ma for the calculations for initial values based on the youngest K-Ar ages of [6] (Table 4). Notwithstanding the poorly constrained age, two main conclusions can be drawn from the data in Fig. (9): (a) the isotope composition of our dyke are clearly different from the CVL basalts, and (b) the basaltic dykes were derived from a slightly enriched mantle source similar to those documented for basalts related to the opening of the southern Atlantic Ocean (e.g. Nigerian Jurassic dykes and Parana Basalts (Fig. 11).

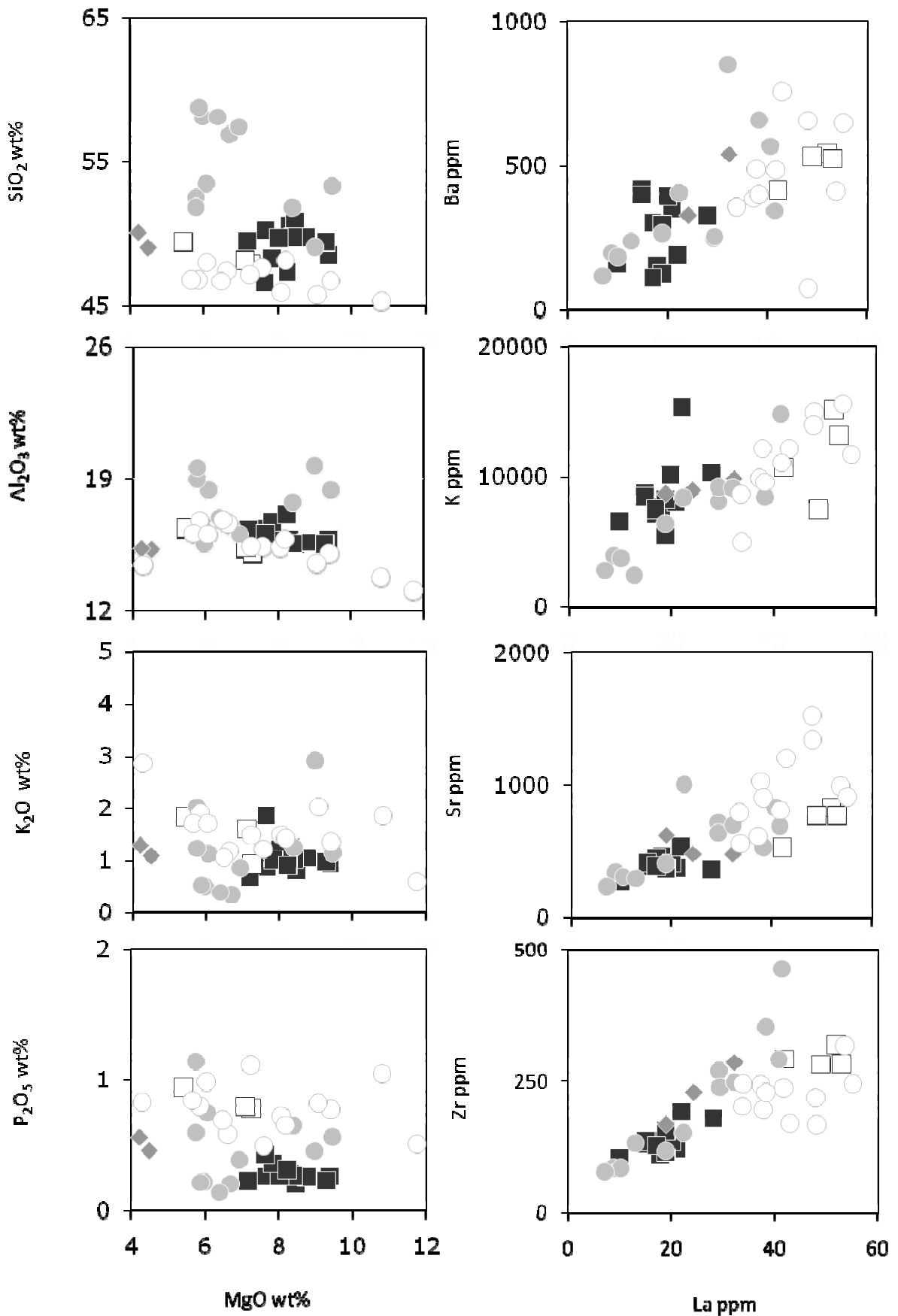


Fig. (7). Variation diagrams of major elements versus MgO and and trace elements versus La. Studied basaltic dykes mostly plot closer to the Benue Through samples [3]. Symbols as in Fig. (6).

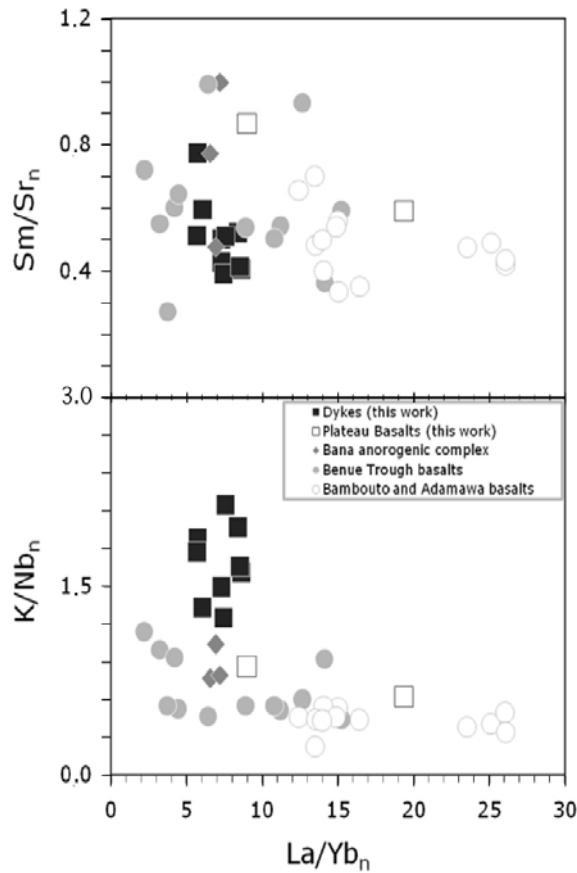


Fig. (8). Sm/Sr_n against La/Yb_n and K/Nb_n against La/Yb_n showing that basalt dykes samples plot closer to basalts from the Benue Through and are distinct from alkaline basalts of the Cameroon Volcanic Line represented here by the plateau basalts and the Bambouto and Adamawa basalts.

DISCUSSION

Major orientations of 10 of the 12 studied dykes the dykes fall in the interval $N30^\circ E$ to $70^\circ E$ which corresponds to the major direction of the Tertiary CVL ($N30^\circ E$) and the Precambrian Adamawa Shear Zone ($70^\circ E$). These two major directions of the dykes fit into a Riedel fracture model [27] with E-W or N-S as the two sets of conjugate shear directions corresponding in a simple shear model to a direction of compression around 40° and extension at ca. 100° . Since this direction is roughly parallel to the African coast in the region and may thus be related to the opening of the Atlantic Ocean.

Geochemically, dykes studied here represent closely associated and relatively evolved magmas ($53 < Mg\# < 59$). Primitive lavas directly derived from the upper mantle ($Mg\#$ of 68–72; [28]) are not observed. Because of their low concentrations in LILE, HFSE and Y compared to those of the Cameroon Volcanic Line (e.g. Plateau basalts, see above), these dykes are similar to tholeiitic dykes in North Cameroon [18], which were thought by [20] to also be unrelated the Cameroon Volcanic Line. Trace element characteristics as shown here much more closely resemble those from tholeiites of the Benue through in Nigeria [17].

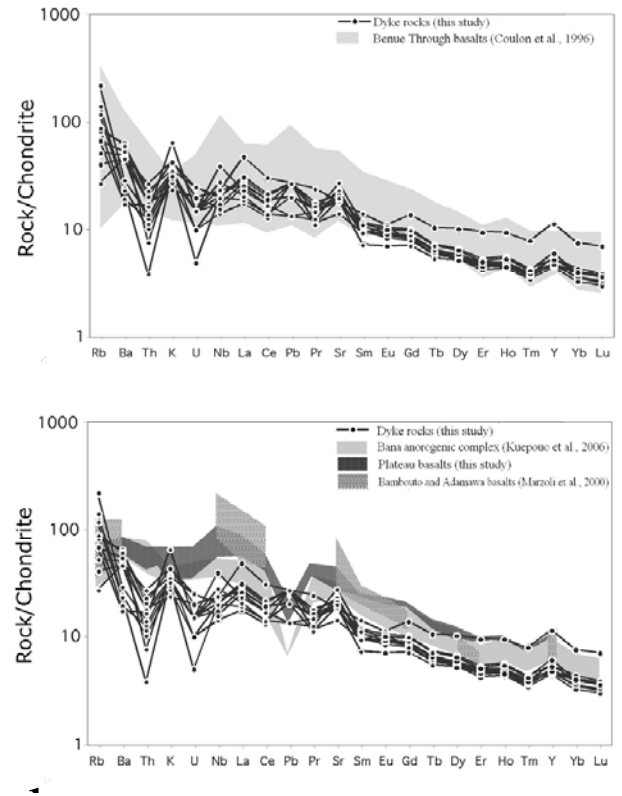


Fig. (9). Spider diagram for incompatible trace elements using the chondrite normalizing values of [26]. Basaltic dykes overlap the Benue Through basalts (a) and are less enriched in incompatible trace elements than representatives of the Cameroon Volcanic Line (b).

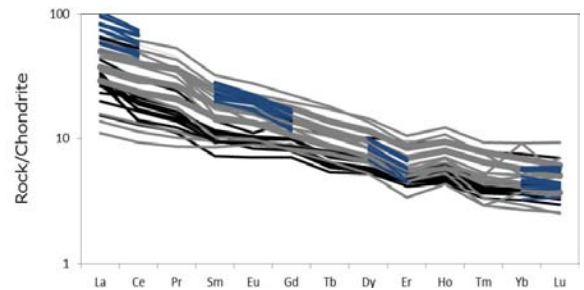


Fig. (10). Chondrite-normalized rare earth element (REE) diagram for dykes samples (black lines) along with fields for Benue through basalts [3] (dark grey lines), Bana anorogenic complex [1] (tick dark grey) and Bambouto [2] (colored lines) showing moderate degrees of REE enrichment. Chondrite normalizing values of [26].

In west-central Africa, magmatism associated with past continental rifting has been dominantly tholeiitic [29–31]. The basaltic dykes share many geochemical features with these basaltic rocks related to the opening of the Atlantic. CIPW compositions are quartz- and hypersthene-normative for all but one sample; a samples (FEM3) of the Manjo area which is olivine normative. This is consistent with a tholeiitic nature, even if modal hypersthene (most consistent with tholeiitic affinity) was not observed in dykes of the Bangangte and Dschang areas. Basalts having similar characteristics are described in the Tertiary CVL volcanism

Table 2. XRF Whole-Rocks Analyses of Basalt Dykes from Bangangte, Dschang, Manjo (FEM1.FEM2.FEM3) and Plateau Basalts from the Bangangte Area. Major Elements are Normalised to 100 LOI-Free. LOI (Loss on Ignition) is Given to Assess the Degree of Alteration

	DMA1	FBB1A	FBB 2	FFD1	FFD2A	FDD2B	FDD 2C	FFD3	FFD4B	FEM 1	FEM2	FEM3	BB 1	BB 6	BB 9	BB 13
	Bangangte			Dschang						Manjo			Plateau basalts Bangangte			
SiO ₂	50.56	50.93	50.21	49.72	48.5	49.71	49.46	49.66	49.44	48.28	47.31	46.57	49.40	48.11	49.85	47.89
TiO ₂	1.68	1.56	1.54	1.51	1.91	1.48	1.38	1.51	1.36	2.05	2.16	2.62	2.74	2.71	3.99	2.73
Al ₂ O ₃	15.82	15.51	16.32	15.57	15.76	15.63	16.25	15.73	15.52	16.68	17.04	16.03	16.35	15.33	15.63	15.04
Fe _{Tot}	10.54	10.74	9.83	11.4	11.39	12.26	11.42	11.33	11.4	11.39	11.5	11.6	11.41	11.99	13.85	12.39
MnO	0.17	0.17	0.12	0.18	0.17	0.21	0.18	0.18	0.18	0.19	0.31	0.2	5.44	7.12	3.78	7.27
MgO	8.31	8.47	7.68	8.41	9.38	8.77	7.18	8.03	9.29	7.85	8.24	7.65	0.17	0.21	0.19	0.21
CaO	8.93	8.64	10.83	9.44	9.26	8.24	10.81	9.48	9.24	9.64	9.82	10.49	7.39	8.40	7.52	8.67
Na ₂ O	2.47	2.99	2.35	2.49	2.43	2.4	2.43	2.6	2.37	2.56	2.41	2.56	4.33	3.74	3.22	4.12
K ₂ O	1.24	0.79	0.86	1.02	0.92	1.05	0.67	1.22	0.97	0.99	0.9	1.85	1.83	1.59	1.35	0.91
P ₂ O ₅	0.29	0.2	0.27	0.26	0.27	0.25	0.22	0.26	0.23	0.36	0.31	0.43	0.94	0.80	0.63	0.78
Total	100	100	100	100	100	100	100	100	100	100	100	100	100	100	100	100
LOI	n.a.	3.87	3.84	6.78	4.07	4.71	3.93	5.50	3.89	4.87	6.18	3.31	0.94	0.81	0.69	0.89
Mg#	0.58	0.58	0.58	0.57	0.59	0.56	0.53	0.56	0.59	0.55	0.56	0.54	0.46	0.51	0.33	0.51
<i>ppm (XRF)</i>																
Ba	323	160	300	399	152	416	298	391	349	125	114	189	539	525	413	530
Rb	31	84	16	53	70	49	24	53	40	52	40	131	41	38	25	37
Th	2.1	0.8	0.9	1.8	0.3	0.6	1.4	1.6	1.4	1	1.3	1.1	5.1	5	3.2	4.5
Sr	359	278	446	413	463	391	366	419	373	369	388	538	829	769	529	769
Nb	15	9.2	13.1	13.1	13	12.9	10.2	12.9	11.2	18.1	15.4	25.4	66.9	68.2	34.4	67.8
Zr	180	107	136	137	110	131	114	136	121	155	129	193	320	283	294	284
Y	48.6	20.3	19.7	20.6	19.2	19.9	19.4	20.4	19.7	23.5	22.7	25.9	29.4	33.9	42.8	34
Co	53	46	57	50	52	50	47	50	54	42	49	45	36	42	38	46
Cr	409	398	372	347	385	352	350	347	381	285	349	195	80	174	9	181
Cu	56	57	66	64	63	63	70	58	63	72	69	62	38	49	30	53
Ga	19	20	19	19	19	18	18	19	18	20	23	20	24	20	26	20
Ni	146	159	209	173	176	186	114	153	179	115	145	88	65	108	25	129
Pb	4	4	4	4	2	3	4	4	3	3	3	2	2	3	3	2
V	206	196	190	189	209	185	186	189	181	224	245	278	153	179	162	183
Zn	103	103	88	95	94	92	89	94	92	87	89	85	1390	16	164	119
U	0.4	0.2	0.1	0.3	0.5	0.2	0.3	0.4	0.5	0.3	0.3	0.3	1.3	1.0	1.2	0.7
<i>REE ppm (ICPMS)</i>						XRF						XRF				
La	30.7	11.28	18.84	19.92	12.18	15	15.84	19.81	17.4	16.48	14.88	21.85	52	53	42	49
Ce	50.33	21.62	33.41	35.65	23.49	38	28.69	35.54	31.4	31.81	27.84	41.35	96	91	71	95
Pr	6.1	2.87	4.13	4.49	3.12		3.65	4.45	3.91	4.13	3.69	5.29	11.51		8.7	
Nd	26.1	14.04	17.92	19.48	15.06	19	16.06	19.31	17.22	18.88	17.28	23.46	48	46	39	47
Sm	5.66	3.81	3.89	4.32	3.84	39	3.74	4.35	3.96	4.71	4.53	5.42	10.4	8.3	8.2	8.8
Eu	1.7	1.4	1.39	1.42	1.37		1.26	1.41	1.28	1.61	1.53	1.91	3.39		3.07	
Gd	7.43	4.85	4.51	4.7	4.47		4.29	4.83	4.34	5.46	5.29	6.17	10.01		10.85	
Tb	1.03	0.62	0.58	0.62	0.59		0.6	0.64	0.58	0.72	0.7	0.8	1.13		1.36	
Dy	6.87	3.72	3.66	3.93	3.59		3.72	3.94	3.65	4.48	4.3	4.98	6.31		8.16	
Ho	1.4	0.68	0.68	0.74	0.65		0.71	0.74	0.7	0.83	0.8	0.9	1.02		1.47	
Er	4.14	1.93	1.97	2.14	1.82		2.07	2.15	2.01	2.32	2.2	2.54	2.79		4.1	
Tm	0.53	0.24	0.25	0.27	0.23		0.26	0.27	0.25	0.29	0.28	0.31	0.3		0.51	
Yb	3.31	1.5	1.58	1.79	1.42		1.76	1.79	1.7	1.9	1.75	2.04	1.83		3.17	
Lu	0.47	0.21	0.22	0.25	0.2		0.24	0.25	0.24	0.26	0.24	0.29	0.25		0.44	

Table 3. Trace Elements Ratios Compared with OIB End-Members, N-MORB, PM and Average Continental Crust from [32]

	Sm/Nd	Zr/Nb	Ba/Th	Th/La	Ba/La	Ba/Nb	K/Nb
DMA1	0.21	12.0	153.8	0.08	11.5	21.5	686.3
FBB1A	0.27	11.6	200.0	0.08	16.0	17.4	708.9
FBB2	0.27	8.5	506.7	0.02	8.4	117	589.5
FFD1	0.27	10.4	333.3	0.05	17.7	22.9	546.3
FFD2A	0.26	10.5	221.7	0.12	26.6	30.5	645.0
FDD2B	0.23	10.2	693.3	0.04	27.7	32.3	678.3
FDD2C	0.22	10.8	249.3	0.07	16.6	31.2	716.3
FFD3	0.24	11.2	212.9	0.07	15.7	29.2	547.3
FFD4B	0.24	10.5	244.4	0.08	19.6	30.3	788.3
FEM1	0.31	8.6	125.0	0.05	6.6	6.9	453.6
FEM2	0.23	8.3	87.7	0.08	6.7	7.4	486.2
FEM3	0.23	7.6	171.8	0.05	8.6	7.4	603.3
<i>References values from Weaver et al. (1991)</i>							
Chondrite	0.33						
Upper Crust	0.17						
HIMU-min		2.7	39	0.1	6.2		
HIMU-max		5.5	85	0.2	9.3		
EM1-min		3.5	80	0.1	11.3		
EM1-max		13.1	204	0.2	19.1		
EM2-min		4.4	57	0.1	7.3		
EM2-max		7.8	105	0.2	13.5		
N-MORB		30	60	4	4.3		
Primitive mantle		14.8	77	0.1	9		
Average cont. crust		16.2	124	0.2	54		

Table 4. Initial Ratios for $^{87}\text{Sr}/^{86}\text{Sr}$ and $^{143}\text{Nd}/^{144}\text{Nd}$ Calculated for $t = 150$ Ma (See Text for Further Explanation)

Samples	Rb ppm	Sr ppm	$^{87}\text{Sr}/^{86}\text{Sr}$	2 SE	$^{87}\text{Rb}/^{86}\text{Sr}$	$(^{87}\text{Sr}/^{86}\text{Sr})_{150\text{Ma}}$	Sm ppm	Nd ppm	$^{143}\text{Nd}/^{144}\text{Nd}$	2SE	$^{147}\text{Sm}/^{144}\text{Nd}$	$(^{143}\text{Nd}/^{144}\text{Nd})_{150\text{Ma}}$
FFD2a	53	413	0.706273	0.00001	0.3712	0.705481	4.9	19	0.512223	0.000006	0.2579	0.511970
FFD2c	40	373	0.706128	0.000012	0.3102	0.705611	3.7	17	0.512227	0.000005	0.1325	0.512097
FFD3	24	366	0.705379	0.000012	0.1897	0.704974	3.9	16	0.512245	0.000006	0.1484	0.512099
FFD4b	53	419	0.706799	0.000012	0.3659	0.706018	4.6	19	0.512232	0.000008	0.1474	0.512087

of the region in the Bana anorogenic complex [15], the widely distributed plateau basalts in the Bayangam [32] and Fouban [33] region. Thus, in terms of major elements and petrographic compositions alone, it is difficult to prove or disprove a genetic similarity between the dykes investigated in this study and the older Tertiary Volcanics of the Cameroon Volcanic Line.

Trace elements patterns and isotope ratios are more conclusive and clearly rule out similarities (and thus genetic relationships) between the studied dykes and the Cameroon Volcanic Line. Rather, these dyke rocks show trace element

patterns from tholeiites of the southern part of the Benue through in Nigeria [3], which is located at the same latitudes as the dykes studied here. These basalts were thought to be of plume origin [3] and to have erupted during a period of crustal thinning (by 10 km or more) during the opening of the South Atlantic Ocean [34]. Their similarity with dyke rocks in Cameroon, the presumed synchronicity and the wide distribution of these related volcanic rocks suggest a much larger area of lithospheric thinning and mantle melting related to the opening of the south Atlantic bordering Central Africa.

CONCLUSION

This work has documented olivine-bearing basaltic dykes of tholeiitic to transitional rift-related character over a large area in southern Cameroon. There are two main geodynamic events in the area to which these dykes potentially could be related: (a) the opening of the Central Atlantic, and; (b) the initial phase of building up of the Cameroon Volcanic Line. Trace element characteristics and Sr- and Nd isotope data clearly rule out a genetic relation to Cameroon Volcanic Line magma sources and rather document similarities to pre-Tertiary volcanic rocks of the Benue Through in Nigeria. This igneous activity that occurred during the opening of the Equatorial Atlantic was apparently much more widely distributed. Further investigations of magma compositions and ages of dykes injection should thus bear important clues on the timing and process of Atlantic rifting.

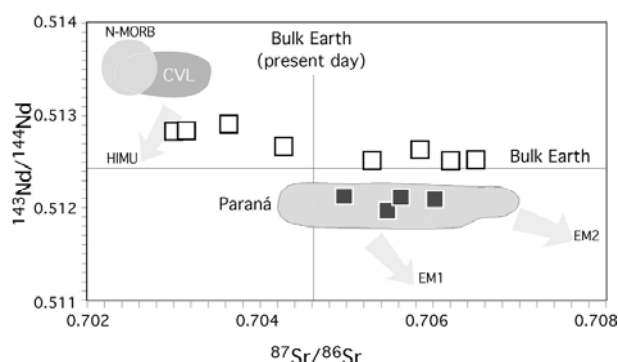


Fig. (11). ¹⁴³Nd/¹⁴⁴Nd vs ⁸⁷Sr/⁸⁶Sr ratios for basalt dykes of the Dschang area at 150 Ma. CVL: Cameroon Volcanic Line. Fields for CVL and Parana are after [3]. Symbols: black squares. basalt dykes (this work); open squares. Benue through basalts [3].

ACKNOWLEDGEMENTS

This work was funded by the German Science Foundation (DFG project Wo362/37-1). G. Hartman, A. Kronz and K. Simon are appreciated for their analytical support.

CONFLICT OF INTEREST

The authors confirm that this article content has no conflict of interest.

REFERENCES

[1] Kuepou G, Tchouankoue JP, Nagao T, Sato H. Transitional tholeiitic basalts in the Tertiary Bana volcano-plutonic complex, Cameroon Line. *J Afr Earth Sci* 2006; 45: 318-32.

[2] Marzoli A, Renne PR, Piccirillo EM, *et al.* The Cameroon Volcanic Line Revisited: Petrogenesis of continental basaltic magmas from lithospheric and asthenospheric mantle sources. *J Petrol* 2000; 41: 87-109.

[3] Coulon C, Vidal P, Dupuy C, Boudin P, *et al.* The Mesozoic to Early Cenozoic Magmatism of the Benue Through (Nigeria): Geochemical Evidence for the Involvement of the St. Helena Plume. *J Petrol* 1996; 37: 1341-58.

[4] Weeksteen G. Carte géologique de reconnaissance du territoire du Cameroun au 1/500000 et notice explicative, feuille Douala-Est. Dir. Mines et Géologie. Yaoundé-Cameroun: Imprimerie Nationale 1957.

[5] Dumort JC. Explanatory notes on the sheet Douala West. Reconnaissance geology map of Cameroon at scale 1/500000. Yaounde-Cameroun: National Printing House 1968.

[6] Tchouankoue JP. Geochronology of the Precambrian basement of West-Cameroon: evidence of a major Paleoproterozoic/Neoproterozoic crustal boundary in Cameroon and its prolongation in North-East Brazil. Doctoral thesis. Cameroon: University of Yaounde I. 2005; p. 133.

[7] Van Schmus WR, Brito Neves BB, Hackspacher P, Babinski M. U/Pb and Sm/Nd geochronologic studies of the eastern Borbomera province, northeastern Brazil: initial conclusions. *J South Am Earth Sci* 1995; 8: 267-88.

[8] Toteu SF, Van Schmus WR, Penaye J, Michard A. New U–Pb and Sm–Nd data from north-central Cameroon and its bearing on the pre-Pan African history of central Africa. *Precambrian Res* 2001; 108: 45-73.

[9] Brito Neves BB, Van Schmus WR, Fetter A. North-western Africa-North-eastern Brazil major tectonic links and correlation problems. *J Afr Earth Sci* 2002; 34: 275-8.

[10] Njiekak G, Dorr W, Tchouankoue JP. U-Pb zircon and microfabric data of (Meta) granitoids of Western Cameroon: Constraints on the timing of pluton emplacement and deformation in the Pan-African belt of Central Africa. *Lithos* 2008; 102: 460-77.

[11] Tchouankoue JP. The Bangangte syenite: A Pan-African complex with intermediate characters: petrology and geochemistry. Doctorate of Third Cycle thesis. Cameroon: University of Yaounde 1992; p.160.

[12] Kwekam M. The Pan-African pluton of Fomopea (West Cameroon): Structural Framework-Petrology-Geochemistry-geodynamic interpretation. Doctorate of Third Cycle Thesis. Cameroon: University of Yaounde 1993; p. 154.

[13] Tchouankoue JP, Ghogomu RT, Tchoua FM. Comparative study of two plutons within atectonic granitoids in Cameroon. *Ann Fac Sci Yaounde* 1994; 3: 166-75.

[14] Tagne-Kamga G. The Ngondo Panafrican plutonic complex (West Cameroon): petrogenesis and structure. Doctorate thesis. France: University of Franche-Comte 1994; p. 224.

[15] Talla, V. The Pan-African granite of Batie (West Cameroon): petrology, structure, geochemistry. Doctorate of Third Cycle Thesis. Cameroon: University of Yaounde 1995; p.144.

[16] Nguessi TC. The calc-alkaline complex of Bandja linked to the Pan-African mobile belt of West Cameroon. Doctorate Thesis. Cameroon: University of Nancy I 1995; p. 240.

[17] Ngounouno L, Déruelle B, Montigny R, Demaiffe D. Les camptonites du mont Cameroun, Afrique. *C R Géosci* 2006; 338: 537-44.

[18] Ngounouno I, Deruelle B, Giraud R, Vicat JP. Magmatismes tholeiitique et alcalin des demi-grabens cretaces de Mayo Oulou-Lere et de Babouri-Figuil (Nord du Cameroun-Sud du Tchad) en domaine d’extension continentale. *C R Acad Sci* 2001; 333(1): 201-7.

[19] Ngounouno I, Déruelle B, Demaiffe D, Montigny R. Petrology of the Cenozoic volcanism in the Upper Benue valley, northern Cameroon (Central Africa). *Contrib Mineral Petrol* 2003; 145(1): 87-106.

[20] Deruelle B, Ngounouno I, Demaiffe D. The Cameroon Hot Line (CHL): A unique example of active alkaline intraplate structure in both oceanic and continental lithospheres. *C R Géosci* 2007; 339: 589-600.

[21] Vicat JP, Ngounouno I, Pouclet A. Existence de dykes doléritiques anciens à composition de tholeiites continentales au sein de la province alcaline de la Ligne du Cameroun. Implications sur le contexte géodynamique. *C R Acad Sci Paris* 2001; 332: 243-9.

[22] Njiekak G, Zulauf G, Tchouankoue JP. Brittle deformation of the West Cameroon Highlands (Central part of the Cameroon Line). *Zentralbl Geol Blaontol Tiel* 2003; 2002: 243-65.

[23] Morimoto N, Fabries J, Ferguson IV, *et al.* Nomenclature of pyroxenes. *Am Mineral* 1988; 73: 1123-33.

[24] Le Bas MJ, Le Maitre RW, Streckeisen A, Zanettin B. A chemical classification of volcanic rocks based on the total alkali-silica diagram. *J Petrol* 1986; 27: 745-50.

[25] Irvine TN, Baragar WRA. A guide to the chemical classification of the common rocks. *Can J Earth Sci* 1971; 8: 523-48.

[26] McDonough WF, Sun SS. 1995. The composition of the Earth. *Chem Geol* 1915; 120: 223-54.

[27] Moreau C, Regnault JM, Deruelle B, Roineau B. A new tectonic model for the Cameroon line, central Africa. *Tectonophysics* 1987; 141: 317-34.

- [28] Green DH. Compositions of basaltic magmas as indicators of conditions of origin: application to oceanic volcanism. *Phil Trans Roy Soc Lond A* 1971; 268: 707-25.
- [29] Sebai A, Zumbo V, Ferand G, *et al.* $^{40}\text{Ar}/^{39}\text{Ar}$ dating of alkaline and tholeiitic magmatism of Saudi Arabia related to the early Red Sea Rifting. *Earth Planet Sci Lett* 1991; 104: 473-87.
- [30] Fiechtner H, Friedrichsen H, Hammerschmidt K. Geochemistry and geochronology of early Mesozoic tholeiites from central Morocco. *Geol Rundsch* 1992; 81: 15-62.
- [31] Harry DL, Sawyer DS. Basaltic magmatism, mantle plumes and the mechanics of rifting: the Parana flood basalt province of South America. *Geology* 1992; 20: 207-10.
- [32] Fosso J, Menard JJ, Bardinzeff JM, Wandji P, Tchoua FM, Bellon H. Les laves du mont Bangou: une première manifestation volcanique Eocène à affinité transitionnelle de la Ligne de Cameroun. *C R Geosci* 2005; 337: 315-25.
- [33] Moundi A, Menard JJ, Reusser E, Tchoua FM, Dietrich V. Discovery of transitional basalts in th continental sector of the Cameroon Line (Mbam massif , West-Cameroon). *C R Acad Sci* 1996; 32 (IIa): 831-7.
- [34] Tokam KAP, Tabod TC, Nyblade AA, Julia J, Wins DA. Structure of the crust beneath Cameron, West Africa, from the joint inversion of Raleigh waves group velocities and receiver functions. *Geophys J Int* 2010; 183:1061-76.

Received: July 30, 2012

Revised: August 30, 2012

Accepted: September 2, 2012

© Tchouankoue *et al.*; Licensee *Bentham Open*.

This is an open access article licensed under the terms of the Creative Commons Attribution Non-Commercial License (<http://creativecommons.org/licenses/by-nc/3.0/>) which permits unrestricted, non-commercial use, distribution and reproduction in any medium, provided the work is properly cited.